

---

---

# Preparation of a Promising Angiogenesis PET Imaging Agent: $^{68}\text{Ga}$ -Labeled c(RGDyK)-Isothiocyanatobenzyl-1,4,7-Triazacyclononane-1,4,7-Triacetic Acid and Feasibility Studies in Mice

Jae Min Jeong<sup>1</sup>, Mee Kyung Hong<sup>1</sup>, Young Soo Chang<sup>1</sup>, Yun-Sang Lee<sup>1</sup>, Young Joo Kim<sup>1</sup>, Gi Jeong Cheon<sup>2</sup>, Dong Soo Lee<sup>1</sup>, June-Key Chung<sup>1</sup>, and Myung Chul Lee<sup>1</sup>

<sup>1</sup>Department of Nuclear Medicine, Cancer Research Institute College of Medicine, Seoul National University, Seoul, Korea; and

<sup>2</sup>Department of Nuclear Medicine, Korea Institute of Radiological and Medical Sciences, Seoul, Korea

---

Arg-Gly-Asp (RGD) derivatives have been labeled with various radioisotopes for the imaging of angiogenesis in ischemic tissue, in which  $\alpha_v\beta_3$  integrin plays an important role. In this study, cyclic Arg-Gly-Asp-D-Tyr-Lys [c(RGDyK)] was conjugated with 2-(*p*-isothiocyanatobenzyl)-1,4,7-triazacyclononane-1,4,7-triacetic acid (SCN-Bz-NOTA) and then labeled with  $^{68}\text{Ga}$ . The labeled RGD so produced was subjected to an *in vitro* binding assay and *in vivo* biodistribution and PET studies. **Methods:** A mixture of SCN-Bz-NOTA (660 nmol) and c(RGDyK) (600 nmol) in 0.1 M sodium carbonate buffer (pH 9.5) was allowed to react for 20 h at room temperature in the dark for thiourea bond formation. The conjugate obtained was purified by semipreparative high-performance liquid chromatography (HPLC). The purified c(RGDyK)-SCN-Bz-NOTA (NOTA-RGD) was then labeled with  $^{68}\text{Ga}$  from a  $^{68}\text{Ge}/^{68}\text{Ga}$  generator and purified by semipreparative HPLC. A competitive binding assay for c(RGDyK) and NOTA-RGD was performed with  $^{125}\text{I}$ -c(RGDyK) as a radioligand and  $\alpha_v\beta_3$  integrin-coated plates as a solid phase.  $^{68}\text{Ga}$ -NOTA-RGD (0.222 MBq/100  $\mu\text{L}$ ) was injected, through a tail vein, into mice with hind limb ischemia and into mice bearing human colon cancer SNU-C4 xenografts. Biodistribution and imaging studies were performed at 1 and 2 h after injection. **Results:** The labeling of NOTA-RGD with  $^{68}\text{Ga}$  was straightforward. The  $K_i$  values of c(RGDyK) and NOTA-RGD were 1.3 and 1.9 nM, respectively. In the biodistribution study, the mean  $\pm$  SD uptake of  $^{68}\text{Ga}$ -NOTA-RGD by ischemic muscles was  $1.6 \pm 0.2$  percentage injected dose per gram (%ID/g); this uptake was significantly blocked by cold c(RGDyK) to  $0.6 \pm 0.3$  %ID/g ( $P < 0.01$ ). Tumor uptake was  $5.1 \pm 1.0$  %ID/g, and the tumor-to-blood ratio was  $10.3 \pm 4.8$ . Small-animal PET revealed rapid excretion through the urine and high levels of tumor and kidney uptake. **Conclusion:** Stable  $^{68}\text{Ga}$ -NOTA-RGD was obtained in a straightforward manner at a high yield and showed a high affinity for  $\alpha_v\beta_3$  integrin, specific uptake by

angiogenic muscles, a high level of uptake by tumors, and rapid renal excretion.  $^{68}\text{Ga}$ -NOTA-RGD was found to be a promising radioligand for the imaging of angiogenesis.

**Key Words:** integrin; NOTA; gallium; peptide; ischemia; DOTA

**J Nucl Med 2008; 49:830–836**

DOI: 10.2967/jnumed.107.047423

---

**A**ngiogenesis is related to various diseases, such as cancer, arthritis, and psoriasis (1). The binding of  $^{125}\text{I}$ -labeled 3-iodo- $\gamma^5$ -cyclic Arg-Gly-Asp-D-Tyr-Lys [c(RGDyK)] to  $\alpha_v\beta_3$  integrin has been described in the literature for the targeting of angiogenesis (2). However, it has the shortcoming of high gut activity because of hepatobiliary excretion. Various other radiolabeled Arg-Gly-Asp (RGD) derivatives have been developed to improve pharmacokinetics, and the introduction of sugar residues has been found to increase renal excretion and to significantly improve pharmacokinetics (3,4).

Dimerization and multimerization have also been used to improve pharmacokinetics. Dimeric RGD derivatives labeled with  $^{99\text{m}}\text{Tc}$ , which has a 6-h half-life, showed an increased affinity for  $\alpha_v\beta_3$  integrin and favorable pharmacokinetics for imaging (5,6). In another study, dimeric RGD derivatives labeled with  $^{111}\text{In}$  and  $^{90}\text{Y}$  showed potential as cancer imaging and therapeutic agents, respectively (7). In addition, a quantitative study of an  $^{18}\text{F}$ -labeled dimeric RGD derivative with a short half-life proved its suitability for PET (8). A further study with multimeric (e.g., tetrameric and octameric) RGD derivatives revealed their feasibility as imaging or therapeutic agents after labeling with a radionuclide with a long half-life, such as  $^{64}\text{Cu}$  (half-life = 12.7 h, 40%  $\beta^-$  [656 keV], 19%  $\beta^+$  [600 keV], 38% electron capture [EC]) (9).

The importance of  $^{68}\text{Ga}$  for clinical PET has increased recently (10).  $^{68}\text{Ga}$  is a positron emitter with a short half-life

---

Received Sep. 18, 2007; revision accepted Jan. 30, 2008.

For correspondence or reprints contact: Jae Min Jeong, Department of Nuclear Medicine, Seoul National University Hospital, 28 Yungun-dong, Jongro-gu, Seoul 110-744, Korea.

E-mail: jmjng@snu.ac.kr

COPYRIGHT © 2008 by the Society of Nuclear Medicine, Inc.

(67.6 min) and can be produced by use of a  $^{68}\text{Ge}/^{68}\text{Ga}$  generator (11–13). Its short half-life and hydrophilic nature are adequate for the labeling of small peptides with rapid renal clearance for PET. A highly effective concentration method for generator-eluted  $^{68}\text{Ga}$  was reported for efficient peptide labeling (14,15). In addition,  $^{68}\text{Ga}$  has a great advantage for PET over other cyclotron-produced positron emitters because it can be obtained economically by use of a commercially available  $^{68}\text{Ge}/^{68}\text{Ga}$  generator. The parent nuclide  $^{68}\text{Ge}$  has a long half-life (270.8 d), allowing its use as a generator for more than 1 year.

In the present study, we used a 1,4,7-triazacyclononane-1,4,7-triacetic acid (NOTA)-based bifunctional chelating agent to label an RGD peptide with  $^{68}\text{Ga}$ . NOTA is a 9-member cyclic compound and has been reported to form a highly stable neutral complex with gallium, which is inert even in 6N nitric acid (16). Functionalized NOTA derivatives suitable for conjugation with proteins or peptides have been reported by many researchers (17–20), and the feasibility of NOTA derivatives as bifunctional chelating agents for the labeling of monoclonal antibodies or somatostatin with  $^{67}\text{Ga}$  has been demonstrated by a biodistribution study in mice (21,22).

We conjugated c(RGDyK) with 2-(*p*-isothiocyanatobenzyl)-NOTA (SCN-Bz-NOTA) to produce a c(RGDyK)-SCN-Bz-NOTA (NOTA-RGD) conjugate (Fig. 1). We then labeled this conjugate with  $^{68}\text{Ga}$  and tested the feasibility of  $^{68}\text{Ga}$ -NOTA-RGD for the imaging of angiogenesis in mice with induced hind limb hypoxia and in mice bearing tumor xenografts.

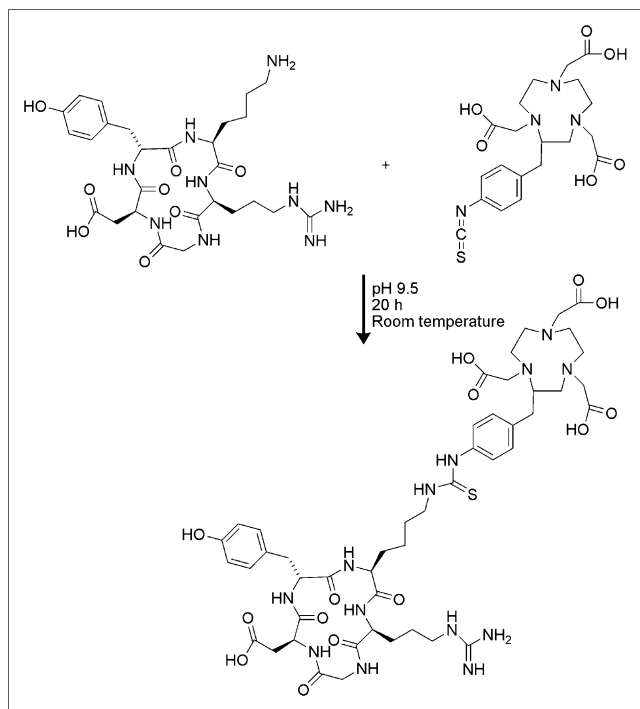


**FIGURE 1.** Synthesis of NOTA-RGD. Molar equivalents of c(RGDyK) and SCN-Bz-NOTA were allowed to react in sodium carbonate buffer (pH 9.5) for 20 h at room temperature.

## MATERIALS AND METHODS

### General

An Agilent 1100 series high-performance liquid chromatography (HPLC) apparatus was used for purifying synthesized and labeled compounds. An XTerra column was purchased from Waters. Mass spectra were obtained with an API-3000 spectrometer (Applied Biosystems), and  $^1\text{H}$  nuclear magnetic resonance (NMR) spectra were obtained with a 300-MHz, AL 300 FT NMR spectrometer (JEOL Ltd.). A  $^{68}\text{Ge}/^{68}\text{Ga}$  generator was purchased from Cyclotron Co. A DU650 spectrophotometer was obtained from Beckman Coulter Inc. A Bio-Scan system 200 imaging scanner was used to scan radioactivity distributions on instant thin-layer chromatography (ITLC) plates. A Cobra II  $\gamma$ -scintillation counter (Packard Canberra Co.) was used for the detection of radioactivity. A rodent R4 microPET scanner (Concorde Microsystems Inc.) was used for animal PET.

SCN-Bz-NOTA and c(RGDyK) were purchased from Futurechem. ITLC-silica gel [SG] was purchased from Gelman. Falcon 96-well polyvinyl chloride (PVC) plates were purchased from Becton Dickinson.  $^{125}\text{I}$ -NaI was purchased from NEN. All of the other reagents were purchased from Sigma-Aldrich.

### Synthesis of NOTA-RGD and Cold Gallium-NOTA-RGD

A mixture of SCN-Bz-NOTA (660 nmol, 0.3 mg) and c(RGDyK) (600 nmol, 0.37 mg) in 0.1 M sodium carbonate buffer (pH 9.5) was allowed to react for 20 h at room temperature in the dark (Fig. 1). The reaction mixture was purified by HPLC (XTerra preparative column RP18; 10  $\times$  250 mm; 0%–100% ethanol gradient in 0.01% trifluoroacetic acid from 0 to 30 min; flow rate, 3 mL/min), and the NOTA-RGD peak sample was collected at a retention time of 13.2 min. The pooled NOTA-RGD fractions were analyzed by liquid chromatography–electrospray ionization–mass spectrometry:  $m/z$ ,  $[\text{M}+\text{H}]^+ = 1,071$  (calculated for molecular formula  $\text{C}_{47}\text{H}_{67}\text{N}_{13}\text{O}_{14}\text{S}$ ; 1,069.5). The  $^1\text{H}$  NMR spectrum was obtained after drying under vacuum and redissolving in  $\text{D}_2\text{O}$ :  $\delta$  0.78–1.90 (m, 9H), 2.57–3.65 (m, 34H), 4.00–4.05 (d, 2H), 4.18 (bs, 2H), 4.37 (bs, 2H), 6.57 (bs, 2H), 6.89 (d, 2H), 7.07 (d, 2H), and 7.19 (bs, 2H).

The molar absorptivity of NOTA-RGD at 240 nm in water was measured and found to be  $14,300 \text{ M}^{-1}$ .

Gallium(III) chloride (110 nmol, 19.4  $\mu\text{g}$  in 10  $\mu\text{L}$  of water) was added to NOTA-RGD (20 nmol, 21.4  $\mu\text{g}$  in 0.1 mL of water), and the mixture was incubated for 10 min at room temperature. The reaction mixture was analyzed with the same HPLC conditions as those described earlier.

### Labeling with $^{68}\text{Ga}$

$^{68}\text{Ga}$  was eluted from the  $^{68}\text{Ge}/^{68}\text{Ga}$  generator with 0.1N HCl.  $^{68}\text{Ga}$  (740 MBq in 1 mL of 0.1N HCl) was added to a NOTA-RGD solution (30 nmol in 0.1 mL of water) prepared as described earlier, and the pH was adjusted to 6.0 with a 7% sodium bicarbonate solution. After incubation for 10 min at room temperature, labeling efficiencies were checked by ITLC-SG with 0.1 M citric acid and 0.1 M sodium carbonate as eluting solvents, in which the  $R_f$  values of  $^{68}\text{Ga}$ -NOTA-RGD were 0.0 and 1.0, respectively, whereas those of free  $^{68}\text{Ga}$  were 1.0 and 0.0, respectively. The radiolabeled product was purified by HPLC (XTerra preparative column RP18; 10  $\times$  250 mm; 0%–100% ethanol gradient in 0.01% trifluoroacetic acid from 0 to 30 min; flow rate, 3 mL/min), and the  $^{68}\text{Ga}$ -NOTA-RGD peak sample was collected at a retention time of 12.5 min. The radioactivity and the

optical density at 240 nm of the peak fraction were measured, and the specific activity was calculated from the data. The stability was checked by ITLC after incubation for 4 h at room temperature.

### In Vitro Binding Assay

Human  $\alpha_v\beta_3$  integrin was obtained from human placenta by affinity chromatography according to a published method (23,24). Preparation and dissociation constant determination for  $^{125}\text{I}$ -iodo-c(RGDyK) were reported previously (25). In brief,  $^{125}\text{I}$ -iodo-c(RGDyK) was prepared with the chloramine-T method at a yield of 92.6% and a radiochemical purity (after HPLC purification) of greater than 99%. The specific activity of  $^{125}\text{I}$ -iodo-c(RGDyK) was 80.7 GBq/ $\mu\text{mol}$ . Its dissociation constant and maximum binding values for human  $\alpha_v\beta_3$  integrin (as a coating on plates), as determined by saturated-binding experiments, were 1.013 and 0.093 nM, respectively (25). The  $K_i$  of NOTA-RGD was determined as previously described (25). In brief, an  $\alpha_v\beta_3$  integrin solution (1  $\mu\text{g}/100 \mu\text{L}$ ; purified from human placenta) in 50 mM sodium carbonate buffer (pH 9.6) was used to coat 96-well PVC plates. The radioligand  $^{125}\text{I}$ -c(RGDyK) (3.7 kBq) was then used in a competitive binding assay with 9 pM–9  $\mu\text{M}$  c(RGDyK) and NOTA-RGD in 20 mM Tris-HCl buffer (pH 7.4) containing 150 mM NaCl, 1 mM  $\text{CaCl}_2$ , 1 mM  $\text{MnCl}_2$ , and 1 mM  $\text{MgCl}_2$  for 2 h at 4°C. Wells were washed 4 times with 200  $\mu\text{L}$  of phosphate-buffered saline containing 1% bovine serum albumin. Wells were cut out with scissors, and counts were obtained with a  $\gamma$ -scintillation counter. The experiment was repeated 3 times in duplicate.

### Biodistribution in Mice with Hind Limb Ischemia

All animal experiments were performed with the approval of the Institutional Animal Care and Use Committee of the Clinical Research Institute at Seoul National University Hospital (an Association for Assessment and Accreditation of Laboratory Animal Care–accredited facility). In addition, National Research Council guidelines for the care and use of laboratory animals (revised in 1996) were observed throughout.

For the creation of an angiogenesis model, unilateral hind limb ischemia was induced in male ICR mice (8–10 wk old) by left femoral artery ablation (25,26). On day 7 after the induction of ischemia,  $^{68}\text{Ga}$ -NOTA-RGD (0.22 MBq/0.1 mL) was injected through a tail vein. For blocking studies, a mixture of c(RGDyK) (3 mg/kg) and  $^{68}\text{Ga}$ -NOTA-RGD (0.15 MBq/0.1 mL) was injected intravenously into mice with hind limb ischemia ( $31.9 \pm 2.5$  [mean  $\pm$  SD] g,  $n = 9$ ). Mice were sacrificed by cervical dislocation at 1 h after injection; bilateral hind limb thigh muscles, blood, and other organs were separated immediately and weighed; and counts were obtained with a  $\gamma$ -scintillation counter. Results are expressed as the percentage injected dose per gram of tissue (%ID/g).

### Biodistribution in Mice Bearing Colon Cancer Xenografts

The human colon cancer cell line SNU-C4 was grown in RPMI 1640 medium containing 10% fetal bovine serum and harvested with trypsin. Cells were washed with 10 mL of phosphate-buffered saline by centrifugation (3,000 rpm). Each nude mouse (male,  $19.4 \pm 1.3$  g) was injected subcutaneously with  $5 \times 10^6$  SNU-C4 cells in the right shoulder. After 17 d,  $^{68}\text{Ga}$ -NOTA-RGD (0.15 MBq/0.1 mL) was injected intravenously into each xenograft-bearing mouse. Mice were sacrificed at 1 h after injection, and biodistribution was investigated as described earlier.

### PET of Mice Bearing Xenografts

Nude mice received xenografts of SNU-C4 cells as described earlier, and tumors were grown for 14 d.  $^{68}\text{Ga}$ -NOTA-RGD (16 MBq/0.1 mL) was then injected either with or without cold c(RGDyK) (60  $\mu\text{g}$ ) through a tail vein. Mice were anesthetized with 2% isoflurane at 2 h after injection, and PET images were obtained for 20 min (static images). PET studies were performed with a dedicated small-animal PET scanner (rodent R4 microPET scanner; Concorde Microsystems Inc.). The acquired 3-dimensional emission data were reconstructed to temporally framed sinograms by use of Fourier rebinning and an ordered-subsets expectation maximization reconstruction algorithm without attenuation correction. Image visualization was performed with ASIPro software (Concorde Microsystems Inc.). For the PET scans, mice were kept under 2% isoflurane anesthesia and temperature was maintained at 30°C with a carbon pad as described previously (27).

## RESULTS

### Synthesis

The synthesis of NOTA-RGD is shown in Figure 1. The conjugated product NOTA-RGD was confirmed by mass spectrometry and NMR spectroscopy. HPLC purification of the reaction mixture was straightforward because of large differences between the retention times of the starting materials and the product; the retention times of c(RGDyK), NOTA-RGD, and SCN-Bz-NOTA were 9.7, 13.2, and 18.4 min, respectively. The NOTA-RGD peak moved forward to 12.4 min after chelation with cold gallium (Supplemental Fig. 1; supplemental materials are available online only at <http://jnm.snmjournals.org>).

### Radiolabeling

The entire labeling procedure, including the purification step, was completed within 30 min. The  $^{68}\text{Ga}$ -NOTA-RGD produced was analyzed by ITLC. For this analysis, ITLC-SG plates were eluted with 0.1 M citric acid; the  $R_f$  values of free  $^{68}\text{Ga}$  and  $^{68}\text{Ga}$ -NOTA-RGD were 1.0 and 0.0, respectively. On the other hand, the  $R_f$  values changed markedly when ITLC-SG plates were eluted with 0.1 M sodium carbonate; free  $^{68}\text{Ga}$  remained at the origin, and  $^{68}\text{Ga}$ -NOTA-RGD moved with the solvent front. The labeling efficiency was 89%, and no free  $^{68}\text{Ga}$  was found after purification (Supplemental Fig. 2).

$^{68}\text{Ga}$ -NOTA-RGD showed an earlier retention time (12.6 min) than unlabeled NOTA-RGD in preparative HPLC (Supplemental Fig. 3). The free  $^{68}\text{Ga}$  peak appeared at 4.2 min, and the specific activity of the purified  $^{68}\text{Ga}$ -NOTA-RGD was 17.4 GBq/ $\mu\text{mol}$ . Moreover, the  $^{68}\text{Ga}$ -NOTA-RGD preparation was found to be stable for more than 4 h at room temperature.

The net charge of  $^{68}\text{Ga}$ -NOTA-RGD was determined to be positive by paper electrophoresis (Supplemental Fig. 4).

### In Vitro Binding Assay

$^{125}\text{I}$ -Iodo-c(RGDyK) was used in a competitive binding assay with c(RGDyK) and NOTA-RGD, and the resulting inhibition curves showed similar patterns (Fig. 2). The  $K_i$  values of c(RGDyK) and NOTA-RGD were  $1.4 \pm 0.3$  and

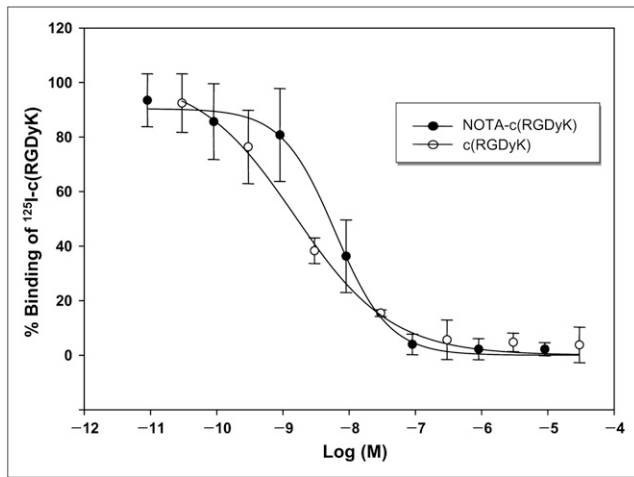


**FIGURE 2.** Inhibition of  $^{125}\text{I}$ -c(RGDyK) binding to human  $\alpha_v\beta_3$  integrin immobilized on PVC plates by c(RGDyK) and by NOTA-RGD.  $K_i$  values of c(RGDyK) and NOTA-RGD were 1.3 and 1.9 nM, respectively. Experiment was repeated 3 times in duplicate.

$3.6 \pm 2.4$  nM, respectively, indicating that the conjugation of NOTA to c(RGDyK) did not substantially affect the binding affinity for c(RGDyK) and  $\alpha_v\beta_3$  integrin.

#### Biodistribution in Hind Limb Ischemia Model

Biodistribution was investigated with the mouse hind limb ischemia model at 7 d after left femoral artery ablation (Fig. 3). The highest level of  $^{68}\text{Ga}$ -NOTA-RGD uptake was found in the kidneys ( $5.1 \pm 1.8$  %ID/g at 1 h); the levels of uptake in the liver ( $2.6 \pm 0.6$  %ID/g at 1 h) and intestine ( $2.0 \pm 0.3$  %ID/g) were significantly lower ( $P < 0.01$ ), indicating the predominance of the renal excretion route. Ischemic hind limb muscle ( $1.6 \pm 0.2$  %ID/g at 1 h) showed a significantly higher level of uptake ( $P < 0.01$ ) than normal hind limb muscle ( $0.5 \pm 0.1$  %ID/g at 1 h). The uptake of  $^{68}\text{Ga}$ -NOTA-RGD by hind limb ischemic

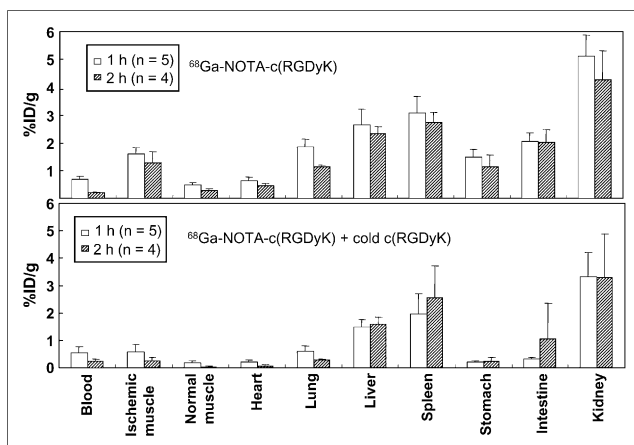


**FIGURE 3.** Biodistribution of  $^{68}\text{Ga}$ -NOTA-RGD without and with cold c(RGDyK) coinjection in mice with induced hind limb ischemia. Values represent mean %ID/g, and error bars represent SD.

muscle decreased significantly ( $P < 0.01$ ) when cold c(RGDyK) was coinjected, indicating that  $^{68}\text{Ga}$ -NOTA-RGD binding was specifically blocked by cold c(RGDyK).

#### Biodistribution in Tumor Xenograft Model

Biodistribution was investigated with human colon cancer SNU-C4 xenograft-bearing nude mice at 17 d after the xenograft procedure (Fig. 4). The highest levels of  $^{68}\text{Ga}$ -NOTA-RGD uptake were found in the kidneys ( $5.3 \pm 1.3$  %ID/g at 1 h) and then in tumors ( $5.1 \pm 1.0$  %ID/g at 1 h) (Fig. 4). Again, significantly lower levels of uptake in the liver ( $2.1 \pm 0.5$  %ID/g at 1 h) and intestine ( $2.3 \pm 0.3$  %ID/g at 1 h) than in the kidneys indicated the predominance of the renal excretion route (Fig. 4). The tumor-to-blood ratio ( $10.3 \pm 4.8$ ) and the tumor-to-muscle ratio ( $9.3 \pm 3.9$ ) were very high.

#### Imaging in Tumor Xenograft Model

A small-animal PET study was performed at 14 d after nude mice received human colon cancer SNU-C4 xenografts (Fig. 5). Images were obtained at 1 and 2 h after  $^{68}\text{Ga}$ -NOTA-RGD was injected either with or without cold c(RGDyK) through a tail vein. A high level of bladder activity at 1 h confirmed rapid renal excretion, which disappeared after urination on 2-h images (Fig. 5A). High levels of uptake were found in tumors and kidneys on 2-h images. The levels of uptake in the liver and intestine were not high, indicating minor hepatobiliary excretion (Fig. 5A). Tumor uptake was significantly blocked by cold c(RGDyK) (Fig. 5B).

#### DISCUSSION

In the present study, a c(RGDyK) derivative was investigated as a potential ligand for imaging angiogenesis, because it was previously shown that cyclic derivatives of RGD, such as c(RGDfK) and c(RGDyK), have a high affinity for  $\alpha_v\beta_3$  integrin (28–30). In terms of preparation, c(RGDyK) and SCN-Bz-NOTA were conjugated by thio-urea bond formation, leaving all 3 carboxyl residues of NOTA intact and available for forming a complex with  $^{68}\text{Ga}$ . It was previously shown that  $\text{Ga}^{3+}$  complexes with the 3 carboxyl and 3 tertiary amine residues of NOTA to

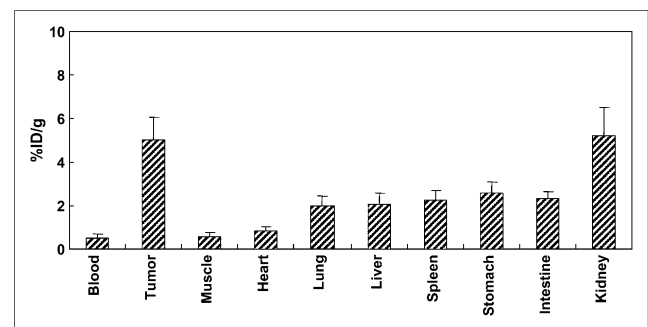


**FIGURE 4.** Biodistribution of  $^{68}\text{Ga}$ -NOTA-RGD in mice bearing SNU-C4 xenografts at 1 h after injection through tail vein. Values represent mean %ID/g, and error bars represent SD.

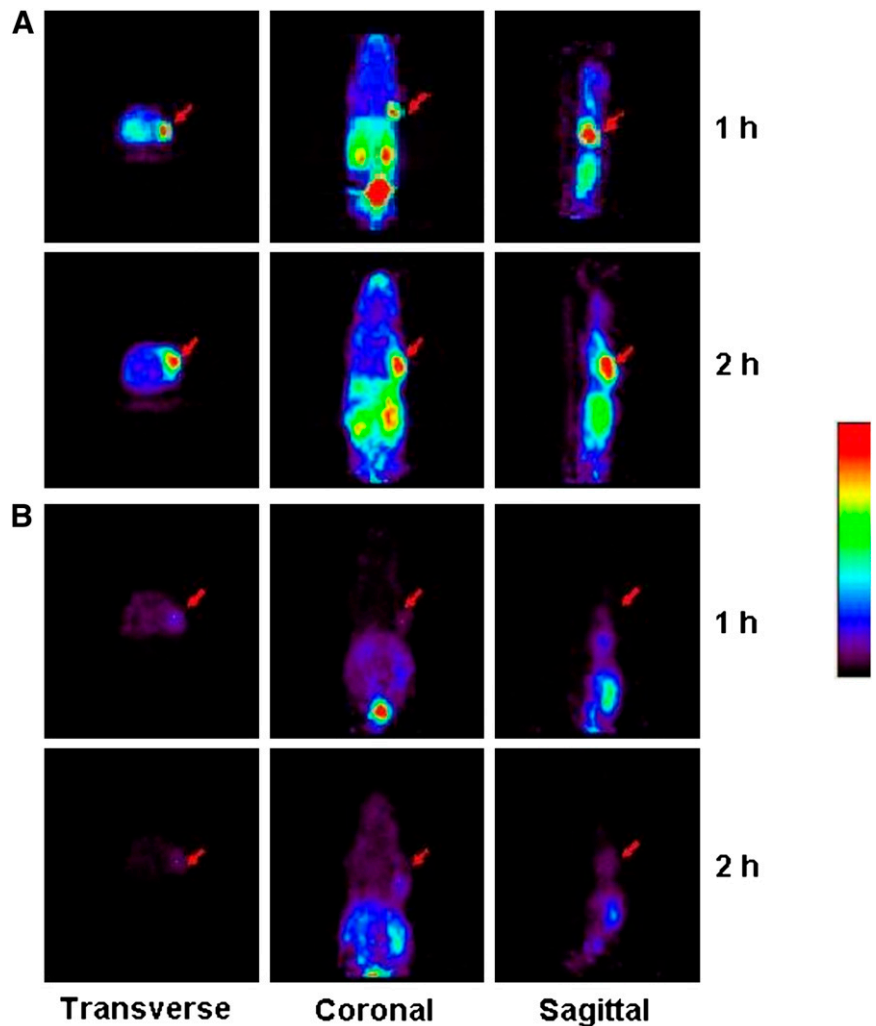


**FIGURE 5.** Small-animal PET of  $^{68}\text{Ga}$ -NOTA-RGD injected into mice bearing SNU-C4 xenografts at 1 and 2 h after injection without cold c(RGDyK) (A) or with cold c(RGDyK) ( $60\ \mu\text{g}$ ) (B). Images at 1 h were taken before micturition, and images at 2 h were taken after micturition. Arrows indicate tumor positions. Acquisition time was 20 min.

form an octahedral chelate with some trigonal–prismatic properties (31).

After purification by preparative HPLC, NOTA-RGD was labeled with  $^{68}\text{Ga}$ , which was eluted from a titanium dioxide–based  $^{68}\text{Ge}/^{68}\text{Ga}$  generator. More than 70% of the  $^{68}\text{Ga}$  activity was eluted in the second fraction of 1-mL samples from the generator. Labeling was performed at room temperature, whereas in previous studies,  $90^\circ\text{C}$  was used for the  $^{68}\text{Ga}$  labeling of 1,4,7,10-tetraazacyclododecane-*N,N',N'',N'''*-tetraacetic acid (DOTA)–conjugated peptides (14,32). Nevertheless, because of the high levels of stability of gallium and the NOTA complex, this reaction was possible at room temperature over only 10 min; this reaction time is an attractive feature, especially for the labeling of heat-labile compounds. Although DOTA is more widely used as a bifunctional chelating agent, it is evident that NOTA is more suitable for complex formation with  $\text{Cu}^{2+}$  and  $\text{Ga}^{3+}$ , which have relatively smaller ionic diameters than  $\text{In}^{3+}$  and  $\text{Y}^{3+}$  (the latter 2 form stable complexes with DOTA). Although a  $^{68}\text{Ga}$ -NOTA chelate should be neutral, paper electrophoresis showed that  $^{68}\text{Ga}$ -

NOTA-RGD was positively charged, presumably because of its strongly basic arginine residue (Supplemental Fig. 4). This finding is supported by its lack of movement on acidic ITLC-SG plates when eluted with a citric acid solution. On the other hand, it could move with the solvent front when it was eluted with an  $\text{Na}_2\text{CO}_3$  solution because the positive charge disappeared in the basic solution. Free  $^{68}\text{Ga}$  moved with the solvent front when eluted with a citric acid solution and remained at the origin when eluted with  $\text{Na}_2\text{CO}_3$  because of colloid formation.

$^{18}\text{F}$  is one of the most important positron-emitting candidates for the labeling of RGD derivatives, and various RGD derivatives have been labeled with  $^{18}\text{F}$  for PET.  $^{18}\text{F}$  has a longer half-life than  $^{68}\text{Ga}$ , a property that increases the quality of PET images because a longer half-life allows more nonspecific activity washout. However, in general,  $^{18}\text{F}$  labeling is time-consuming and laborious. The most widely used conventional  $^{18}\text{F}$ -labeling method includes *N*-succinimidyl 4- $^{18}\text{F}$ -fluorobenzoic acid conjugation to amine residues of peptides (4,33–35). A straightforward and rapid  $^{18}\text{F}$ -labeling method using carrier-added  $^{18}\text{F}\text{-F}_2$  gas

has also been described (36). However, its product had low specific activity (32.8 GBq/mmol) and showed a low level of tumor uptake and high levels of nonspecific uptake in the liver, intestine, and kidneys in a mouse biodistribution study. An efficient  $^{18}\text{F}$ -labeling method based on no-carrier-added  $^{18}\text{F}$ -fluoride has also been described. This method was based on oxime formation between  $^{18}\text{F}$ -fluorobenzaldehyde and aminoxy-modified galactosylated cyclic RGD derivatives. The adduct produced showed substantially higher levels of uptake in the liver, kidneys, and tumors than in other tissues (37). Another highly efficient and straightforward labeling method was based on the formation of hydrazone between  $^{18}\text{F}$ -fluorobenzaldehyde and hydrazino-nicotinic acid-conjugated peptides (38). RGD derivatives labeled with this hydrazone formation method showed high specific activity (20.5 GBq/ $\mu\text{mol}$ ) and substantially higher levels of uptake in angiogenic ischemic tissues than in normal tissues (25). However, they also showed high levels of uptake in the liver and intestine because of the hydrophobicity of the fluorobenzene moiety, which is therefore not ideal for whole-body PET because of high nonspecific abdominal activity. Moreover, a comparative study of  $^{18}\text{F}$ -labeled and  $^{64}\text{Cu}$ -labeled RGD derivatives clearly showed that  $^{18}\text{F}$ -labeled compounds were taken up by the liver and excreted into the intestine much faster than  $^{64}\text{Cu}$ -labeled compounds (39). These literature searches led us to conclude that high levels of liver and intestinal uptake of unglycosylated monomeric RGD derivatives labeled with the  $^{18}\text{F}$ -fluorobenzene moiety are attributable to hydrophobicity. In addition,  $^{18}\text{F}$  labeling requires a cyclotron system,  $^{18}\text{O}$ -enriched water, a long irradiation time for  $^{18}\text{F}$  production, and a complicated and time-consuming multistep procedure, all of which incur substantial costs.

Two animal biodistribution models were used in the present study, that is, hind limb ischemia and SNU-C4 (human colon cancer cell line) xenografts. Angiogenesis is known to occur after ischemia lesions as well as during cancer development. The mouse hind limb ischemia model has been used as a means of causing angiogenesis for experimental purposes because of its convenience and reliability (25,26). SNU-C4 xenograft-bearing mice have been used because the solid tumors produced induce angiogenesis. In the present study, we found a significantly higher level of  $^{68}\text{Ga}$ -NOTA-RGD uptake in ischemic muscle than in nonischemic muscle; this uptake was found to be blocked by cold c(RGDyK), indicating specific binding by  $^{68}\text{Ga}$ -NOTA-RGD (Fig. 3).  $^{68}\text{Ga}$ -NOTA-RGD uptake in tumors also was blocked by cold c(RGDyK) in PET studies, further evidence of its specific binding to angiogenic tissue (Fig. 5).

These results concur with those of a previously reported study, except that the liver and intestinal activities significantly decreased when  $^{18}\text{F}$ -labeled c(RGDyK) was used (25). The high liver and intestinal activities were the results of rapid hepatobiliary excretion because of hydrophobicity. The introduction of hydrophilic sugar residues significantly

increased renal excretion and decreased hepatobiliary excretion (3,4). In the present study, increased renal excretion and decreased hepatobiliary excretion were attributable to the hydrophilicity of  $^{68}\text{Ga}$ -NOTA residues, which resembled the hydrophilic nature of sugar residues in a previous report (40).

In the present study, high levels of uptake in tumors and kidneys predominated in biodistribution and imaging studies with human colon cancer SNU-C4 xenograft-bearing nude mice at 1 and 2 h after injection. SNU-C4 cells inoculated into the right shoulder were grown for 14–17 d. Although the level of uptake in the kidneys was high, it is acceptable for a PET agent because it can be easily kept under a hazardous radiation level and will seldom disturb image reading or analysis.

## CONCLUSION

A novel NOTA-RGD conjugate was synthesized, labeled with generator-eluted  $^{68}\text{Ga}$ , and then investigated in vitro and in vivo. First,  $^{68}\text{Ga}$ -NOTA-RGD was produced rapidly at a high-yield with a straightforward method. Second, it was found to be a promising agent for PET imaging of angiogenesis, with high stability, high affinity, high specificity, and excellent pharmacokinetic properties. Finally, it offers significant progress for PET imaging of angiogenesis because of the rapidly growing distribution of  $^{68}\text{Ge}/^{68}\text{Ga}$  generators.

## ACKNOWLEDGMENTS

This work was supported by a Korea Research Foundation grant funded by the Korean Government (MOEHRD, Basic Research Promotion Fund) (KRF-2006-E00414). This work also was supported by a Korea Science and Engineering Foundation grant (KOSEF-2008-00610). This study was presented in part at the 17th International Symposium on Radiopharmaceutical Sciences, April 30–May 4, 2007, Aachen, Germany.

## REFERENCES

1. Carmeliet P, Jain RK. Angiogenesis in cancer and other diseases. *Nature*. 2000;407:249–257.
2. Haubner R, Wester HJ, Reuning U, et al. Radiolabeled  $\alpha_v\beta_3$  integrin antagonists: a new class of tracers for tumor targeting. *J Nucl Med*. 1999;40:1061–1071.
3. Haubner R, Wester HJ, Burkhart F, et al. Glycosylated RGD-containing peptides: tracer for tumor targeting and angiogenesis imaging with improved biokinetics. *J Nucl Med*. 2001;42:326–336.
4. Haubner R, Kuhnast B, Mang C, et al. [ $^{18}\text{F}$ ]Galacto-RGD: synthesis, radiolabeling, metabolic stability, and radiation dose estimates. *Bioconjug Chem*. 2004; 15:61–69.
5. Janssen M, Oyen WJG, Massuger LFA, et al. Comparison of a monomeric and dimeric radiolabeled RGD-peptide for tumor targeting. *Cancer Biother Radiopharm*. 2002;17:641–646.
6. Jia B, Shi J, Yang Z, et al.  $^{99\text{m}}\text{Tc}$ -Labeled cyclic RGDfK dimer: initial evaluation for SPECT imaging of glioma integrin  $\alpha_v\beta_3$  expression. *Bioconjug Chem*. 2006; 17:1069–1076.
7. Janssen ML, Oyen WJ, Dijkgraaf I, et al. Tumor targeting with radiolabeled  $\alpha_v\beta_3$  integrin binding peptides in a nude mouse model. *Cancer Res*. 2002;62: 6146–6151.

8. Zhang X, Xiong Z, Wu Y, et al. Quantitative PET imaging of tumor integrin  $\alpha_v\beta_3$  expression with  $^{18}\text{F}$ -FRGD2. *J Nucl Med.* 2006;47:113–121.
9. Li ZB, Cai W, Cao Q, et al.  $^{64}\text{Cu}$ -Labeled tetrameric and octameric RGD peptides for small-animal PET of tumor  $\alpha_v\beta_3$  integrin expression. *J Nucl Med.* 2007;48:1162–1171.
10. Breeman WA, Verbruggen AM. The  $^{68}\text{Ge}/^{68}\text{Ga}$  generator has high potential, but when can we use  $^{68}\text{Ga}$ -labelled tracers in clinical routine? *Eur J Nucl Med Mol Imaging.* 2007;34:978–981.
11. Ehrhardt GJ, Welch MJ. A new germanium-68/gallium-68 generator. *J Nucl Med.* 1978;19:925–929.
12. Schumacher J, Maier-Borst W. A new  $^{68}\text{Ge}/^{68}\text{Ga}$  radioisotope generator system for production of  $^{68}\text{Ga}$  in dilute HCl. *Int J Appl Radiat Isot.* 1981;32:31–36.
13. Ambe S.  $^{68}\text{Ge}/^{68}\text{Ga}$  generator with alpha-ferric oxide support. *Appl Radiat Isot.* 1988;39:49–51.
14. Meyer GJ, Mäcke H, Schuhmacher J, Knapp WH, Hofmann M.  $^{68}\text{Ga}$ -labelled DOTA-derivatised peptide ligands. *Eur J Nucl Med Mol Imaging.* 2004;31:1097–1104.
15. Zheronosekov KP, Filosofov DV, Baum RP, Aschoff P, Bihl H, Razbash AA. Processing of generator-produced  $^{68}\text{Ga}$  for medical application. *J Nucl Med.* 2007;48:1741–1748.
16. Parker D. Tumor targeting with radiolabeled macrocycle-antibody conjugates. *Chem Soc Rev.* 1990;19:271–291.
17. Cox JPL, Craig AS, Helps IM, et al. Synthesis of C- and N-functionalized derivatives of 1,4,7-triazacyclononane-1,4,7-triacetic acid (NOTA), 1,4,7,10-tetraazacyclododecane-1,4,7,10-tetraacetic acid (DOTA), and diethylenetriaminepentaacetic acid (DTPA): bifunctional complexing agents for the derivatization of antibodies. *J Chem Soc Perkin Trans.* 1990;1:1567–1576.
18. Studer M, Meares CF. Synthesis of novel 1,4,7-triazacyclononane-N,N',N''-triacetic acid derivatives suitable for protein labeling. *Bioconjug Chem.* 1992;3:337–341.
19. McMurry TJ, Brechbiel M, Wu C, Gansow OA. Synthesis of 2-(p-thiocyanatobenzyl)-1,4,7-triazacyclononane-1,4,7-triacetic acid: application of the 4-methoxy-2,3,6-trimethylbenzenesulfonamide protecting group in the synthesis of macrocyclic polyamines. *Bioconjug Chem.* 1993;4:236–245.
20. Brechbiel MW, McMurry TJ, Gansow OA. A direct synthesis of a bifunctional chelating agent for radiolabeling proteins. *Tetrahedron Lett.* 1993;34:3691–3694.
21. Lee J, Garmestani K, Wu C, et al. In vitro and in vivo evaluation of structure-stability relationship of  $^{111}\text{In}$ - and  $^{67}\text{Ga}$ -labeled antibody via 1B4M or C-NOTA chelates. *Nucl Med Biol.* 1997;24:225–230.
22. Eisenwiener KP, Prata MIM, Buschmann I, et al. NODAGATOC, a new chelator-coupled somatostatin analogue labeled with [ $^{67}\text{Ga}$ ] and [ $^{111}\text{In}$ ] for SPECT, PET, and targeted therapeutic applications of somatostatin receptor (hst2) expressing tumors. *Bioconjug Chem.* 2002;13:530–541.
23. Kouns WC, Kirchofer D, Hadvary P, et al. Reversible conformational changes induced in glycoprotein IIb-IIIa by a potent and selective peptidomimetic inhibitor. *Blood.* 1992;80:2539–2547.
24. Pytela R, Pierschbacher MD, Argraves S, Suzuki S, Ruoslahti E. Arginine-glycine-aspartic acid adhesion receptors. *Methods Enzymol.* 1987;144:475–489.
25. Lee YS, Jeong JM, Kim HW, et al. An improved method of  $^{18}\text{F}$  peptide labeling: hydrazone formation with HYNIC-conjugated c(RGDyK). *Nucl Med Biol.* 2006;33:677–683.
26. Lee KH, Jung KH, Song SH, et al. Radiolabeled RGD uptake and  $\alpha_v$  integrin expression is enhanced in ischemic murine hindlimbs. *J Nucl Med.* 2005;46:472–478.
27. Woo SK, Lee TS, Kim KM, Kim JY, Jung JH, Kang JH. Anesthesia condition for  $^{18}\text{F}$ -FDG imaging of lung metastasis tumors using small animal PET. *Nucl Med Biol.* 2008;35:141–148.
28. Aumailley M, Gurrath M, Müller G, Calvete J, Timpl R, Kessler H. Arg-Gly-Asp constrained within cyclic pentapeptides: strong and selective inhibitors of cell adhesion to vitronectin and laminin fragment P1. *FEBS Lett.* 1991;291:50–54.
29. Gurrath M, Müller G, Kessler H, Aumailley M, Timpl R. Conformation activity studies of rationally designed potent anti-adhesive RGD peptides. *Eur J Biochem.* 1992;210:911–921.
30. Pfaff M, Tangemann K, Müller G, et al. Selective recognition of cyclic RGD peptides of NMR defined conformation by  $\alpha_{\text{IIb}}\beta_3$ ,  $\alpha_v\beta_3$  and  $\alpha_5\beta_1$  integrins. *J Biol Chem.* 1994;269:20233–20238.
31. Moore DA, Fanwick PE, Welch MJ. A novel hexachelating amino-thiol and its complex with gallium(III). *Inorg Chem.* 1990;29:672–676.
32. Schuhmacher J, Zhang H, Doll J, et al. GRP receptor-targeted PET of a rat pancreas carcinoma xenograft in nude mice with a  $^{68}\text{Ga}$ -labeled bombesin(6–14) analog. *J Nucl Med.* 2005;46:691–699.
33. Vaidyanathan G, Zalutsky MR. Labeling proteins with fluorine-18 using N-succinimidyl 4-[ $^{18}\text{F}$ ]fluorobenzoate. *Nucl Med Biol.* 1992;19:275–281.
34. Wester HJ, Hamacher K, Stöcklin G. A comparative study of N.C.A. fluorine-18 labeling of proteins via acylation and photochemical conjugation. *Nucl Med Biol.* 1996;23:365–372.
35. Chen X, Park R, Shahinian AH, et al.  $^{18}\text{F}$ -Labeled RGD peptide: initial evaluation for imaging brain tumor angiogenesis. *Nucl Med Biol.* 2004;31:179–189.
36. Ogawa M, Hatano K, Oishi S, et al. Direct electrophilic radiofluorination of a cyclic RGD peptide for in vivo  $\alpha_v\beta_3$  integrin related tumor imaging. *Nucl Med Biol.* 2003;30:1–9.
37. Poethko T, Schottelius M, Thumshirn G, et al. Two-step methodology for high-yield routine radiohalogenation of peptides:  $^{18}\text{F}$ -labeled RGD and octreotide analogs. *J Nucl Med.* 2004;45:892–902.
38. Chang YS, Jeong JM, Lee Y-S, et al. Preparation of  $^{18}\text{F}$ -human serum albumin: a simple and efficient protein labeling method with  $^{18}\text{F}$  using a hydrazone-formation method. *Bioconjug Chem.* 2005;16:1329–1333.
39. Chen X, Park R, Tohme M, Shahinian AH, Bading JR, Conti PS. MicroPET and autoradiographic imaging of breast cancer  $\alpha_v$ -integrin expression using  $^{18}\text{F}$ - and  $^{64}\text{Cu}$ -labeled RGD peptide. *Bioconjug Chem.* 2004;15:41–49.
40. Prante O, Einsiedel J, Haubner R, et al. 3,4,6-Tri-O-acetyl-2-deoxy-2-[ $^{18}\text{F}$ ]fluoroglucopyranosyl phenylthiosulfonate: a thiol-reactive agent for the chemoselective  $^{18}\text{F}$ -glycosylation of peptides. *Bioconjug Chem.* 2007;18:254–262.